We are IntechOpen,
the world's leading publisher of
Open Access books
Built by scientists, for scientists

6,900
Open access books available

186,000
International authors and editors

200M
Downloads

Our authors are among the

154
Countries delivered to

TOP 1%
most cited scientists

12.2%
Contributors from top 500 universities

CLARIVATE ANALYTICS
BOOK CITATION INDEX
INDEXED

WEB OF SCIENCE™

Selection of our books indexed in the Book Citation Index
in Web of Science™ Core Collection (BKCI)

Interested in publishing with us?
Contact book.department@intechopen.com

Dynamic Contrast Enhanced Magnetic Resonance Imaging in Rectal Cancer

Roberta Fusco[1], Mario Sansone[1], Mario Petrillo[2], Antonio Avallone[3],
Paolo Delrio[3] and Antonella Petrillo[3]
[1]*Department of Biomedical, Electronics and Telecommunications Engineering*
University 'Federico II' of Naples
[2]*Department of Radiology, Second University of Naples*
[3]*IRCCS National Cancer Institute, Fondazione Pascale, Naples*
Italy

1. Introduction

In the last few years the clinical management of rectal cancer has become very complex. A wide spectrum of therapeutic options is available. Magnetic Resonance Imaging (MRI) could play a pivotal rule in the prognostic and therapeutic assessment of rectal cancer (Chen et al., 2005).

As known, MRI can provide information about the stage of the disease according to TNM classification focussing on the depth of mesorectal invasion and on lymph node involvement inside and outside the mesorectum (Beets-Tan & Beets, 2004; Gunderson et al., 2004). Due to its intrinsic multiparametricity and multiplanarity MRI is considered the 'gold standard' particularly in differentiating between intramural and extramural disease, and in the management of Locally Advanced Rectal Cancer (LARC) (Beets-Tan & Beets, 2004; Petrillo et al., 2006).

The common use of total mesorectal excision (TME) and the shift from a postoperative to a preoperative chemo-radiotherapy (pre-CRT) approach have substantially reduced the risk of local recurrences, increasing curative resection and the rate of anal sphincter preservation and improving local control and overall survival rates (Avallone et al., 2006; 2011; Delrio et al., 2005; 2003).

Although morphological tumour assessment performed by MRI has been repeatedly shown to be the most accurate modality in evaluating the presence of a positive circumferential resection margin (CRM), MRI is considered not to be conclusive in pre-CRT tumor response evaluation since histopathological downstage is not always associated with tumour effective reduction (Petrillo et al., 2007). The main difficulty regarding post-chemoradiation MRI includes discrimination of active tumour and post-treatment fibrosis, particularly when differentiating stage T2 and stage T3 carcinomas, according to different recurrence and overall survival rates between Low Risk (T1/T2N0) and Intermediate Risk (T3/N0) as reported by Gunderson et al. (2002; 2004).

Previous considerations support a Dynamic Contrast Enhanced-Magnetic Resonance Imaging (DCE-MRI) approach that could gain a renewed role to MRI adding functional data to

the morphological examination. DCE-MRI has been reported by many authors as a tool potentially able to permit an evaluation of pre-CRT effectiveness basing on the strict relationship between tumor growth and angiogenesis (Ceelen et al., 2006; de Lussanet et al., 2005; Kremser et al., 2007).

DCE-MRI is gaining a large consensus as a technique for diagnosis, staging and assessment of therapy response for different types of tumours, due to its capability to detect highly active angiogenesis. It is well known that angiogenesis is a key factor in the growth and dissemination of cancer; characterisation of the angiogenic status of the tumour on an individual patient basis could allow for a more targeted approach to treatment of rectal cancer (Goh et al., 2007; Kapse & Goh, 2009).

More specifically, in the case of rectal cancer, previous trials have provided the proof of principle that inhibition of angiogenesis has the potential to enhance the effectiveness of the treatment for this disease. In vivo imaging techniques capable to assess tumour perfusion have the potential to improve the management of treatment for patients with rectal cancer (Chen et al., 2005; de Vries et al., 2000; 2001; 2003; Kremser et al., 2007).

The aim of this chapter is to review the main issues concerning the assessment of the angiogenic status of rectal cancer by means of DCE-MRI. More specifically, the aim of this chapter is to present:

- a review of the widespread methodologies used for DCE-MRI data acquisition and analysis;

- the main findings of scientific literature concerning DCE-MRI evaluation of rectal cancer.

2. DCE-MRI basis

Cancer can develop in any tissue of the body that contains cells capable of division. The earliest detectable malignant lesions, referred to as *cancer in situ*, are often a few millimeters or less in diameter and at an early stage are commonly avascular. In avascular tumours cellular nutrition depends on diffusion of nutrients and waste materials and places a severe limitation on the size that such a tumour can achieve. The maximum diameter of an avascular solid tumour is approximately $150 - 200 \mu m$, and is governed effectively by the maximum diffusion distance of oxygen. Conversion of a dormant tumour in situ to a more rapidly growing invasive neoplasm, may take several years and is associated with vascularization of the tumour. The development of neo-vascularization within a tumour results from a process known as angiogenesis.

There are positive and negative regulators of angiogenesis. Release of a promoter substance stimulates the endothelial cells of the existing vasculature close to the neoplasia to initiate the formation of solid endothelial sprouts that grow toward the solid tumour (Knopp et al., 1999). Vascular endothelial growth factor (VEGF) also known as vascular permeability factor (VPF), induces angiogenesis and strongly increases microvascular permeability to plasma proteins. As vascular growth factors are released, proteases are also induced to degrade perivascular tissue, allowing the endothelial cells to proliferate and form primitive, immature, and, therefore, leaky vessels (Dor et al., 2001; Guetz et al., 2006). Figure 1 summarizes the main phases of tumor vasculature development.

Therefore, the morphology of the neo-vascular network in tumours can differ significantly from that seen in normal tissue. Tumour vasculature is often highly heterogeneous, and the capillaries are extremely coarse, irregularly constricted or dilated and distorted.
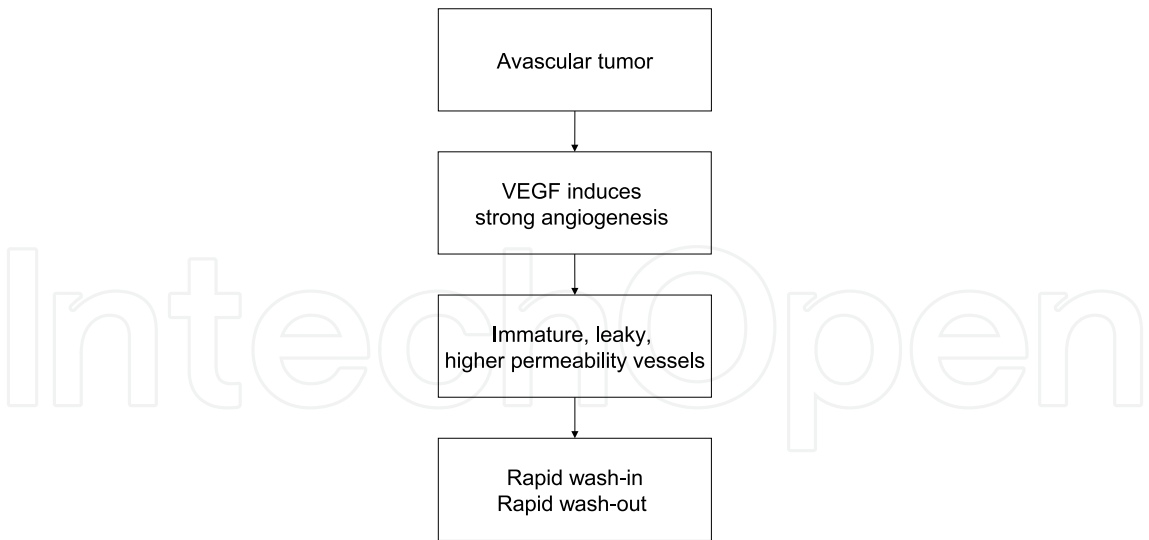
Fig. 1. A summary of the main phases of tumor vasculature development (angiogenesis) and the effects that are measurable by means of DCE-MRI.
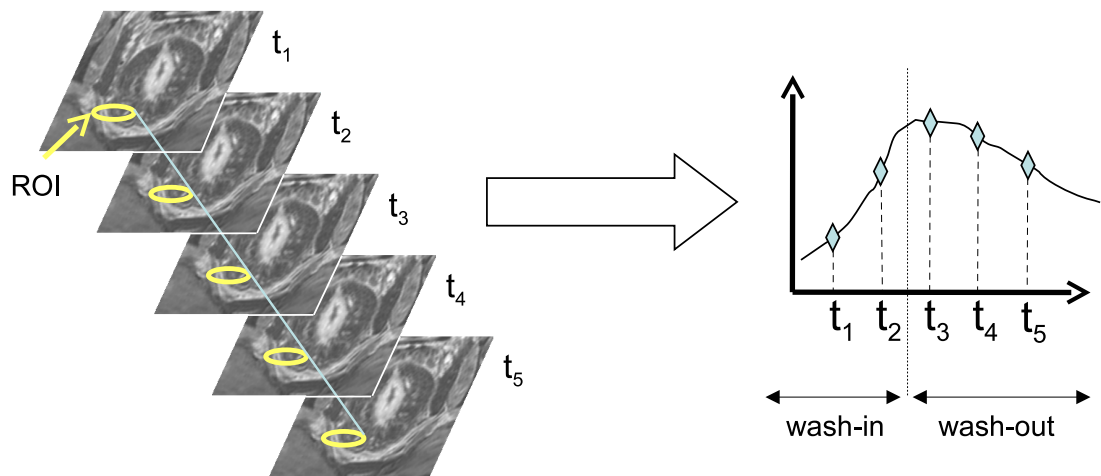

Fig. 2. DCE-MRI in rectal cancer: a series of T_1-weighted images before and after CA injection; the time-intensity curve of the selected region of interest (ROI) is also shown.

Angiogenic inhibitors can reduce both the number of vessels (particularly nonfunctional vessels) and their permeability. Some therapies, such as anti-vascular endothelial growth factor antibody (antiVEGF Ab), are specifically directed against a growth factor (VEGF) and are thought to regulate vascular maturation and permeability (Lichtenbeld et al., 1999).

While avascular tumours are not detectable by MRI (Choyke et al., 2003), DCE-MRI can help to characterise vascularized cancers (Leach et al., 2005). After intravenous injection, the contrast agent (CA) pass through the tumor vasculature and immediately leaks through the vessels walls accumulating in the extravascular extracellular space (EES) because of the concentration gradient (wash-in phase, see fig. 2). Hereafter, CA concentration within plasma will return lower than EES and backflow will occur (wash-out phase). Using specific T_1-weighted pulse sequences the accumulation of CA causes an increase of signal intensity (enhancement) on images (fig. 2). Malignant tumors generally show faster and higher levels of enhancement than is seen in normal tissue. DCE-MRI is currently widely used in the study of tumour angiogenesis and in the development and trial of anti angiogenic drugs.

3. DCE-MRI data acquisition

Several issues of data acquisition should be taken into account when developing protocols for DCE-MRI, both to facilitate the integration of results from multiple institutions and to ensure that the data reflect the underlying physiology as accurately as possible (Ashton, 2010; Evelhoch, 1999; Leach et al., 2005).

In particular, the type of data acquisition affects the data analysis procedure: while semi-quantitative model-free analysis (see section 4) can be performed without accurate measurement of CA concentration, a full model-based approach requires accurate CA quantification.

Key factors affecting DCE-MRI of rectal cancer include: type of contrast agents and the relationship between CA concentration and signal enhancement; constraints concerning spatial and temporal resolution; the impact of patient motion.

3.1 Relationship between contrast agent concentration and signal enhancement

It is generally assumed that the relaxation rate ($R_1 = 1/T_1$) of soft tissues is linearly related to the mean tissue CA concentration (C_T) via the Bloembergen and Solomon equation:

$$R_1 = \frac{1}{T_1} = \frac{1}{T_{1,0}} + r_1 C_T = R_{1,0} + r_1 C_T \tag{1}$$

where $T_{1,0}$ and $R_{1,0}$ are, respectively, the relaxation time and the relaxation rate of the tissue in absence of CA and the proportionality constant r_1 is called 'relaxivity'.

Main properties concerning the relaxivity include: it depends upon the macromolecular environment; it is dependent on the type of macromolecule to which the Gd ion is attached; it decreases with external magnetic field; it increases with temperature; and it is also dependent on the pH of the solution (Stanisz & Henkelman, 2000).

However, most studies assume that r_1 is constant at a given temperature and magnetic field and that it is independent on the tissue environment. The typical value used for r_1, estimated in pure saline water, is 4.5 L/mmol/s per kg of water (Stanisz & Henkelman, 2000).

In typical DCE-MRI experiments, T_1-weighted spoiled gradient-echo sequences are used. In this case the signal intensity S has the following expression (Sourbron, 2010):

$$S = \rho \cdot g \cdot \frac{\sin \alpha \cdot (1 - \exp(-T_R/T_1))}{1 - \cos \alpha \cdot \exp(-T_R/T_1)} \cdot \exp(-T_E/T_2^*) \tag{2}$$

where ρ is the proton density, g is a constant determined by system receiver and image reconstruction settings, α is the flip angle, T_R is the repetition time, T_E is the echo time, T_2^* is the transverse relaxation time taking into account field inhomogeneity.

If it is assumed that Gd ions have no effect on ρ and that the T_E is so short to neglect the influence of T_2 (or, more importantly, changes in T_2^* during the series), then the Gd ions can influence the signal intensity only by means of their effect on T_1 (decrease of T_1). Under these assumptions, and as α approaches $90°$ and $T_R \ll T_1$ the relationship between signal intensity and $1/T_1$ becomes approximately linear:

$$S \approx \rho \cdot g \cdot \frac{T_R}{T_1} \tag{3}$$

this relationship remains approximately valid across a range of values for T_R/T_1 and α.

Therefore, an estimate of CA concentration can be obtained using eq. (1) and eq. (3):

$$[Gd] = \frac{1}{r_1}\left(\frac{1}{T_1} - \frac{1}{T_{1,0}}\right) \approx \frac{S - S_0}{r_1 \cdot \rho \cdot g \cdot T_R} \tag{4}$$

where S_0, S, $T_{1,0}$ and T_1 are the signal intensities and spin-lattice relaxation times before and after administration of contrast agent respectively. The difference $S - S_0$ is called *signal enhancement*.

The difficulty in comparing different studies comes from the nature of g: in fact, the loading of the coil, the receiver settings at the MR console and image reconstruction parameters can be different among several studies.

Therefore, it could be more advantageous to normalise with respect to the pre-contrast signal intensity:

$$[Gd] \approx \frac{S - S_0}{S_0} \frac{1}{r_1 \cdot T_{1,0}}. \tag{5}$$

The quantity $(S - S_0)/S_0$ is called *relative signal enhancement*. Consequently, the concentration of CA is related to both r_1 and $T_{1,0}$ of tissue.

As observed before, the relaxivity r_1 can be considered fixed for soft tissues. As far as the longitudinal relaxation time prior to contrast injection ($T_{1,0}$) it can be easily measured before CA administration using opportune pulse sequences (Collins & Padhani, 2004).

One common method for $T_{1,0}$ estimation is to use several gradient-echo (GRE) images with variable flip angles. In fact, rearranging eq. (2) that equation yields (Parker et al., 1997):

$$Y(\alpha) = X(\alpha) \cdot \exp(-T_R/T_{1,0}) - \rho g(1 - \exp(-T_R/T_{1,0})) \exp(-T_E/T_2^*) \tag{6}$$

where $Y(\alpha) = S_\alpha / \sin\alpha$ and $X(\alpha) = S_\alpha / \tan\alpha$. Hence a plot of $Y(\alpha)$ against $X(\alpha)$ for several (typically three or more) flip angles will result in a straight line and $T_{1,0}$ can be calculated from the slope (via standard linear regression).

3.2 Spatial and temporal resolution

The requirements for temporal and spatial resolution for a particular oncologic application often are in direct conflict. Both the importance for high temporal resolution to accurately characterize contrast kinetics and the need for high spatial resolution to identify distinguishing features of lesion morphology have been investigated in several studies (Cheng, 2008; Dale et al., 2003; Evelhoch, 1999; Henderson et al., 1998).

In general, it can be stated that for an accurate estimation of tracer kinetics parameters, a short interval between samples must be used, especially for the analysis of the wash-in phase. For example, Henderson et al. (1998) found that this interval should be approximately less than 16 s in the case of breast DCE-MRI. In the wash-out phase, this requirement could be relaxed (de Vries et al., 2003; Kremser et al., 2007).

A high temporal resolution can be difficult to obtain because the acquisition of a single volume could require several seconds as a large part of the whole abdomen is scanned. One approach to overcome this problem is to choose a single slice containing the tumor, so that the sampling interval can be maintained below a few seconds (Blomqvist et al., 1998; Ceelen et al., 2006; de Lussanet et al., 2005). However, this approach is not able to manage with the heterogeneity of the tumour (Jackson et al., 2007). An hybrid approach could involve a rapid imaging with low spatial resolution in the wash-in phase while a slow, high-resolution imaging could be adopted in the wash-out phase (de Vries et al., 2000; 2003).
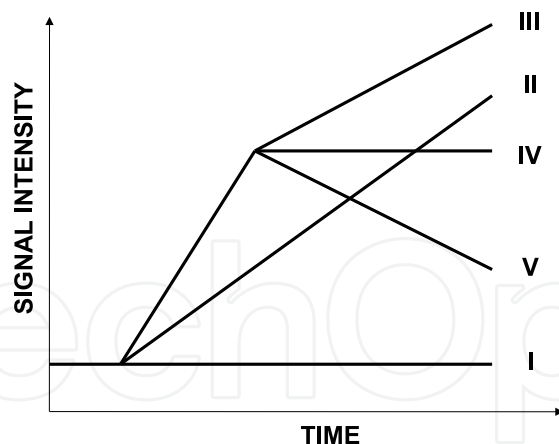
Fig. 3. Classification system for semi-quantitative of the TICs. The level of angiogenesis is supposed to increase with the number of the curve-type: (I) no enhancement; (II) slow sustained enhancement; (III) rapid initial and sustained late enhancement (persistent); (IV) rapid initial and stable late enhancement (plateau); (V) rapid initial and decreasing late enhancement (wash-out). Curves from (I) to (III) are typically associated to normal or benign tissues; type (IV) can be classified as suspicious and (V) as malignant.

3.3 Patient motion

Since the TIC is sampled over several minutes, patient motion can become a serious obstacle to an accurate evaluation of kinetic parameters. Motion correction should be applied before any tracer kinetics analysis is performed (Fei et al., 2002). However, 2D or 3D registration is difficult because the signal intensity of a pixel can change over time both because of spatial displacement and CA absorption. Therefore, DCE-MRI specific methods are currently being developed for simultaneous iterative registration and tracer kinetics analysis (Buonaccorsi et al., 2007; Melbourne et al., 2007; Xiaohua et al., 2005).

4. DCE-MRI data analysis

Different methods for DCE-MRI data analysis have been proposed, ranging from simple semi-quantitative inspection of the time-intensity curves (TICs) to more sophisticated tracer kinetics modelling (Brix et al., 2010; Sourbron, 2010). The different methods were designed to capture the biologically relevant components from the dynamic MR signal and to relate them to the underlying pathophysiological processes taking place in the tissue.

In principle, the derivation of physiological data from DCE-MRI relies on the application of appropriate tracer kinetics models to describe the distribution of contrast media following its systemic administration. However, the application of these techniques is still complex and they cold not be widely available outside specialist centres. In response to this, many semi-quantitative approaches for the classification of enhancement curve shapes have been described and are now in relatively common use in clinical settings.

Both semi-quantitative and full-quantitative data analysis can be performed on a region of interest (ROI) basis or on a pixel-by-pixel basis. We will briefly describe the two approaches.

4.1 Semi-quantitative analysis

Semi-quantitative analysis can help the radiologist in classifying the TIC shape as normal, benign, malignant (see fig. 3). Classification of TICs according to this scheme can achieve very

good diagnostic performance in differentiating malignant from benign lesions as described in the case of breast lesions (Daniel et al., 1998; Kuhl, 2007; Nishiura et al., 2011).

As regards the rectal cancer, many papers explored the possibility to apply a semi-quantitative approach to lesion classification. Different TIC features have been used by the different authors, the aim being to extract as much physiological information as possible.

The approaches can be roughly subdivided in two classes. In a first type of approach, the classification of the TIC is performed by means of several features having, on an intuitive basis, a link with physiological characteristics (see fig. 4). As an example, Tuncbilek et al. (2004) used the maximal relative enhancement within the first minute (MSD_{1min}), the maximal relative enhancement of the entire study (MSD), the steepest slope (WIS_{max}). Similarly, Blomqvist et al. (1998) and Dicle et al. (1999) used MSD and WIS_{max}.

Another approach is to extract TIC features that are associated to tracer kinetics theory (see section 4.2). Within this framework de Lussanet et al. (2005); de Vries et al. (2000; 2001; 2003); Kremser et al. (2007) used, as a first step in quantitative assessment of tumor perfusion, the steepest slope of the TIC during contrast medium uptake (WIS_{max}), and, on the base of the work by Miles (1991) they evaluated the Perfusion Index (PI) as:

$$
\begin{aligned}
PI &= \frac{1}{\sigma_{tumor}} \left[\frac{dC_{tumor}/dt|_{max}}{C_{art}|_{max}} \right] \\
&= \frac{1}{\sigma_{tumor}} \left[\frac{WIS_{max}}{C_p(t)|_{max}} \right]
\end{aligned}
\tag{7}
$$

where σ_{tumor} is tissue density. Although PI is an approximated parameter, it combines two important quantities: tissue perfusion and extraction fraction (Brix et al., 2010; Sourbron, 2010).

When calculated on a pixel-by-pixel basis the above parameters can be displayed graphically as pseudo-coloured maps superimposed on the corresponding morphological MR images (see section 4.3, fig. 7).

Figure 4 shows the most important parameters that have been used in several studies. The definitions of the several quantities are not always in accordance. Therefore we have tried to use a unifying terminology for semi-quantitative parameters (see tab. 1):

TTK time between the beginning of dynamic acquisition and the maximum enhancement;

TWI time between the onset of enhancement and the maximum enhancement;

TWO time between the maximum enhancement and the end of the acquisition;

MSD the maximum signal level with respect to the baseline;

WIS slope of the wash-in phase (increase in signal intensity between enhancement onset and maximum enhancement divided by time to peak);

WOS slope of the wash-out phase (decrease in signal intensity between maximum enhancement and the signal intensity at the end of acquisition divided by time TWO);

WII intercept of the wash-in straight-line with the y-axis;

WOI intercept of the wash-our straight-line with the y-axis;

AUCWI area under gadolinium curve in the was-in phase;

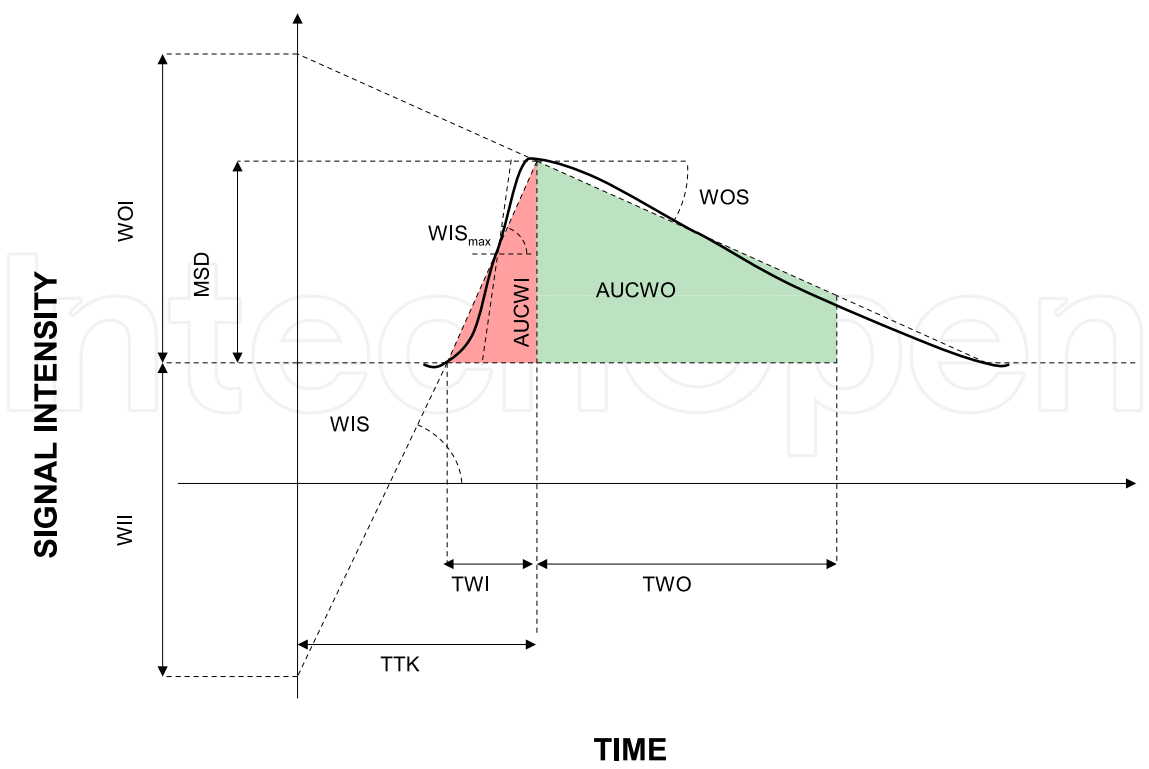**AUCWO** are under gadolinium curve in the wash-out phase;

Fig. 4. Semi-quantitative analysis: illustration of the parameters calculated from the TIC. See table 1 for definition of terms.

Parameter	Definition
TTK	Time To Knee
TWI	Time of Wash-In
TWO	Time of Wash-Out
WII	Wash-In Intercept
WOI	Wash-Out Intercept
WIS	Wash-In slope
WOS	Wash-Out slope
MSD	Maximum Signal Difference
AUCWI	Area Under Wash-In
AUCWO	Area Under Wash-Out

Table 1. Semi-quantitative analysis: definition of terms in fig. 4

4.2 Tracer kinetics modelling

The flow of CA within the tissue of interest can be described using compartmental modelling. Different tracer kinetics modelling approaches have been proposed (Brix et al., 2010; Sourbron, 2010). The most widespread one is the two-compartments model (Tofts, 1997). The advantage of tracer kinetics modelling over semi-quantitative analysis is that it provides an estimate of physiological parameters directly related to vessels permeability and to blood flow (and therefore to the angiogenic status of the tissues).

In order to model CA kinetics in terms of physiologically meaningful parameters we first need to define the elements within the tissue and the functional processes that affect the distribution of the tracer. It is customary to represent the tissue as comprising three or four compartments (fig. 5). Major compartments are: the vascular plasma space, the extra-cellular extra-vascular
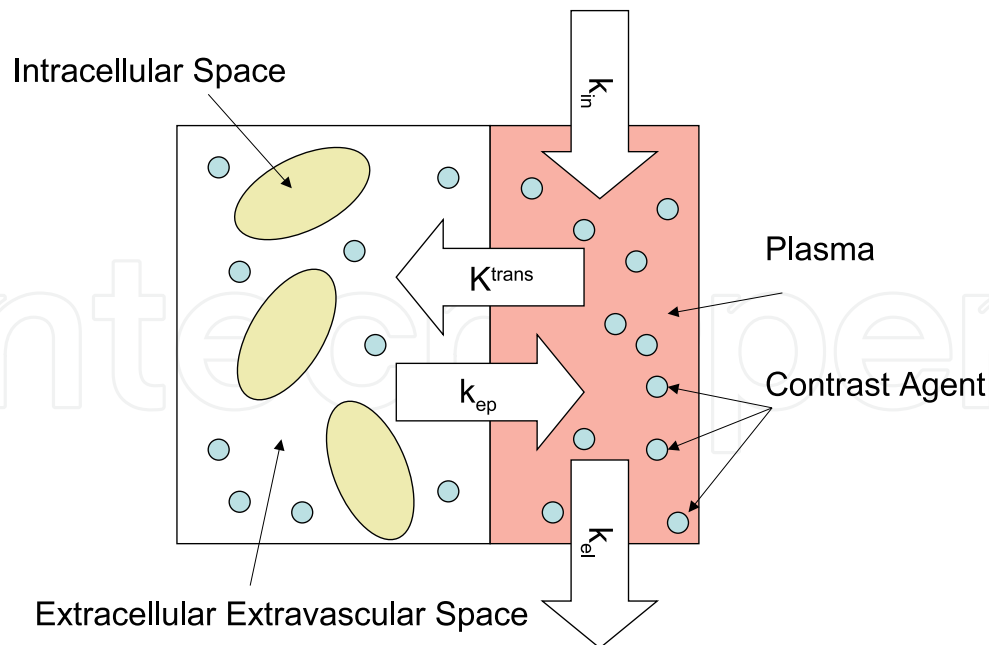
Fig. 5. Major compartments and functional variables involved in the distribution of the contrast agent in the tissue.

space (EES), and the intracellular space. A fourth tissue component forms a catch-all for all the other microscopic tissue components, such as membranes, fibrous tissues, etc.

All clinically utilised MRI contrast agents, and most experimental agents, do not pass into the intracellular space of the tissue, due to their size, inertness, and non-lipophilicity, making the intra-cellular space un-probable using DCE-MRI; for this reason, the intra-cellular and 'other' volumes are usually lumped together as a loosely defined 'intra-cellular' space.

We will indicate the quantities associated to the EES, plasma and intra-cellular compartments with the subscripts e, p and i respectively. The quantities associated to the whole tissue will be marked by a subscript T. The volume occupied by the different compartments may be expressed either as an absolute value (V_e, V_i, V_p, V_T) or as fractions (v_e, v_i, v_p) of V_T. They must satisfy the constraint:

$$v_e + v_p + v_i = 1. \tag{8}$$

All the models make some basic assumptions related to concepts in tracer kinetics. The most important are: the *linearity* of the tissue (the flux of CA between compartments is proportional to the difference of CA concentrations in the two compartments); the *stationarity* of the tissue (the parameters describing the compartments are constant during data acquisition); and the tissue is formed of *well-mixed compartments* (a compartment is said to be well-mixed when the CA immediately distributes over the whole compartmental volume). Under these assumptions the rate of wash-in and wash-out of the CA in the EES can be described by a modified general rate equation (Kety, 1951):

$$v_e \frac{dC_e}{dt} = K^{trans}(C_p(t) - C_e(t)), \tag{9}$$

where C_e and C_p are the CA concentrations [mmol/L] in V_e and V_p respectively; K^{trans} [min^{-1}] is the volume transfer constant between V_p and V_e (see fig. 5) (Tofts, 1997).

There exist a fundamental relationship between K^{trans} and v_e (Tofts et al., 1999):

$$k_{ep} = K^{trans}/v_e, \tag{10}$$

where k_{ep} is the *rate constant* (see fig. 5). The rate constant can be derived from the *shape* of the TIC.

The other two parameters in fig. 5 represent the input function from the injection of gadolinium based contrast (k_{in}) and the clearance rate (k_{el}) (Choyke et al., 2003).

Both blood plasma flow and blood perfusion (capillary permeability) contribute to the value of K^{trans}. If the flow of CA to the tissue is large, K^{trans} is dominated by the capillary wall permeability (permeability surface area, *PS*); if the delivery of CA to the tissue is insufficient, blood perfusion will be the dominant factor, and K^{trans} will be proportional to the blood flow F (volume of blood per unit time):

$$K^{trans} = F \cdot E \tag{11}$$

where E is the extraction fraction of the tracer $E = 1 - \exp(-\frac{PS}{F})$ (PS is the permeability surface area product).

The relationships described above form the basis of the models used to describe contrast agent kinetics by a number of researchers, and the conventions for the names and symbols used are now generally accepted (Tofts et al., 1999).

In normal tissues, the vascular volume is a small fraction $v_p \approx 0$ of the total tissue volume V_T (approximately 5% , although it can be considerably higher in some tissues), and it is sometimes assumed (largely as a matter of convenience) that the tracer concentration in the tissue as a whole, C_T, is not influenced to a large degree by the concentration in the vessels (i.e. $C_T = v_p C_p + v_e C_e \simeq v_e C_e$).

While this assumption is acceptable in abnormalities with small increase in blood volume, that are located in tissues with a relatively low normal blood volume, it is not valid in many contexts, especially because blood volume can largely increase in tumours.

Perhaps the most straightforward approach is to extend eq. 9 to include the concentration of contrast agent in the blood plasma, giving $C_T = v_p C_p + v_e C_e$. Using this relationship and eq. 9 we have the extended Tofts' model (see fig. 6):

$$C_T(t) = v_p C_p(t) + K^{trans} \int_0^t C_p(\tau) \exp\left(-\frac{K^{trans}}{v_e}(t-\tau) \right) d\tau, \tag{12}$$

More comprehensive models, such as the one proposed by St Lawrence & Lee (1998) can allow direct quantification of flow (F), extraction fraction (E), v_e and mean capillary transit time (*MTT*). Here, rather than defining a composite parameter K^{trans}, it is possible to separately estimate F and PS (permeability surface area product). As this model has many parameters, successful application requires a high temporal resolution and an accurate measurement of C_T, which limits its application in clinical trials. The tissue concentration is given by the following equation (St Lawrence & Lee, 1998):

$$C_T(t) = F \int_0^{MTT} C_p(t-u)du + E \cdot F \int_{MTT}^t C_p(u)e^{-\frac{E \cdot F}{v_e}(t-u-MTT)}du \tag{13}$$

In general, the aim of the compartmental analysis is to estimate the parameters K^{trans}, v_p and v_e from DCE-MRI data (Leach et al., 2005). This problem can be seen either as a *system identification* problem or as a *non linear regression* problem (Sourbron, 2010). The limited scope of this chapter does not allow for a deep description of these techniques. We will instead

discuss in further detail an important issue that is prominent whichever approach is used: the influence of $C_p(t)$, the arterial input function (AIF).

4.2.1 Influence of the arterial input function

>From eq. (12) it is clear that the C_T can be seen as the output of a linear system whose impulse response is determined by the tracer kinetics parameters K^{trans} ad v_e and whose input is the AIF. Therefore, errors in estimation of AIF can seriously affect the parameters estimates.

AIF can be obtained by direct measurement of blood flux (Yang et al., 2004). For example, Larsson et al. (1996) utilised an AIF measured from blood samples drawn from the brachial artery at intervals of 15 s during the DCE-MRI data acquisition. This method is not suitable for clinical practice and other approaches have been proposed.

One of the simplest methods was proposed by Brix et al. (1991): they assumed that AIF followed a mono-exponential model and included it as a third parameter directly into the TIC model (se fig. 6 (b)). Another approach for modelling of arterial flux was based on population parameters: the early application proposed by Tofts (1997) assumed a bi-exponential form of the AIF as previously found in normal population (Weinmann et al., 1984). Also multi-exponential modelling by means of nonlinear fitting of arterial flux measured directly on the images on a patient by patient basis has been investigated (Larsson et al., 1996).

Exponential modelling has shown to be only applicable when the sampling rate is relatively slow and there is a negligible plasma fraction. When the plasma fraction is non-negligible, this approach tends to over-estimate the volume transfer constant K_{trans}. To overcome this problem, Parker et al. (2006) measured a high temporal resolution population AIF on a large number of individuals and estimated the parameters of a sophisticated model. Later, Orton et al. (2008) proposed a computationally efficient version of this model decomposing the input function into a bolus model and a body transfer function:

$$C_p(t) = A_B t e^{-\mu_B t} + A_G (e^{-\mu_G t} - e^{-\mu_B t}). \tag{14}$$

A similar model for AIF has been previously proposed by Simpson et al. (1999):

$$C_p(t) = A \cdot t \cdot e^{-t \cdot B} + C[1 - e^{-t \cdot D}] \cdot e^{-t \cdot E} \tag{15}$$

where A, B, C, D, E were estimated on an individual basis.

Also, other approaches based on reference tissues have been proposed (Walker-Samuel et al., 2007; Yankeelov et al., 2005). The development of many analysis methods has proceeded in tandem with specific data acquisition programmes, and the modelling assumptions frequently reflected limitations imposed by the data. Care must therefore be taken in applying these methods in settings other than those originally intended and in comparing apparently compatible results from different studies using different models and/or data acquisitions.

4.3 ROI vs pixel-by-pixel

Region Of Interest (ROI)-based analysis involves the selection (manual or [semi]-automatic) of a ROI and subsequently averaging of the TICs over the ROI (fig. 2). The data-analysis is then applied on the averaged TIC. ROI-based analysis has the advantages of speed and ease of use; moreover, if the ROI is opportunely chosen the SNR can be increased. However, it has the disadvantage of intra-observer variability; moreover, ROI-based analysis could be unable to catch heterogeneity within the tumour (Jackson et al., 2007). Further, inappropriate selection

(a)

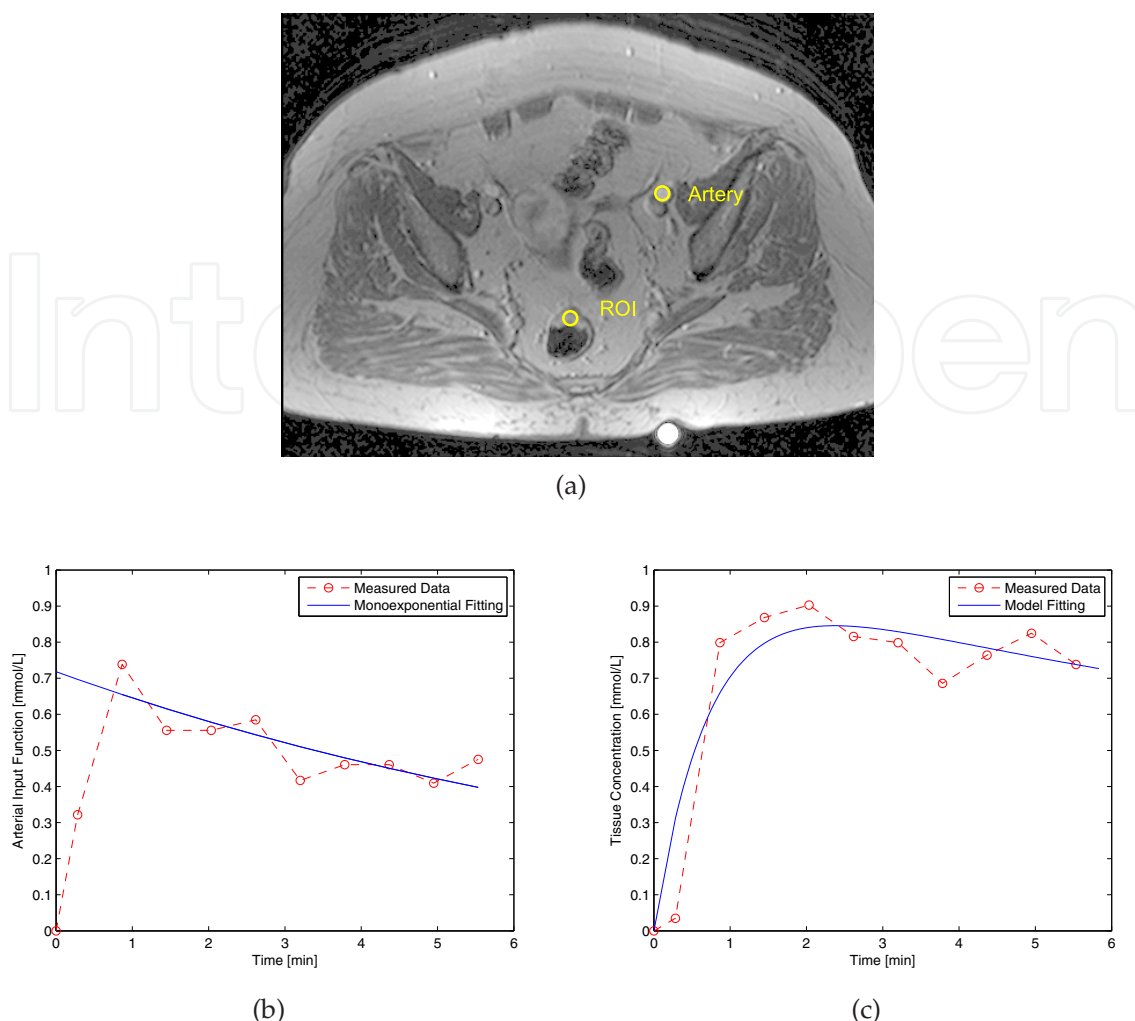(b)   (c)

Fig. 6. a) The ROIs selected by an expert radiologist on the artery and on the tissue of interest; b) the time intensity curve of AIF; c) Curve fitting using the Tofts model.

of the ROI, so that it includes both enhancing and necrotic or non-enhancing components of the tumour, could give misleading interpretation.

These shortcomings can be addressed applying the data-analysis on a pixel-by-pixel basis obtaining a map for each chosen parameter (Fig. 7). Pixel by pixel analysis deals specifically with tumour heterogeneity and potentially provides a far wider range of information concerning tumour behaviour than is available from ROI analysis. Summary values within a ROI can subsequently be obtained averaging the parametric map. Unfortunately, the use of parametric images imposes significant further demands on the acquisition and analysis techniques. In particular, the use of pixel by pixel analysis assumes that there is negligible motion at the spatial resolution of the individual voxel.

An hybrid approach consists in using parametric maps for ROI selection and subsequent application of data analysis to the ROI. This approach can potentially benefit from both ROI-based and pixel-by-pixel processing (Sourbron, 2010).

Also, semi-automatic approaches for model-based segmentation of DCE-MRI images are currently being developed (Buonaccorsi et al., 2007; Kelm et al., 2009; Sansone et al., 2011; Schmid et al., 2006; Xiaohua et al., 2005)
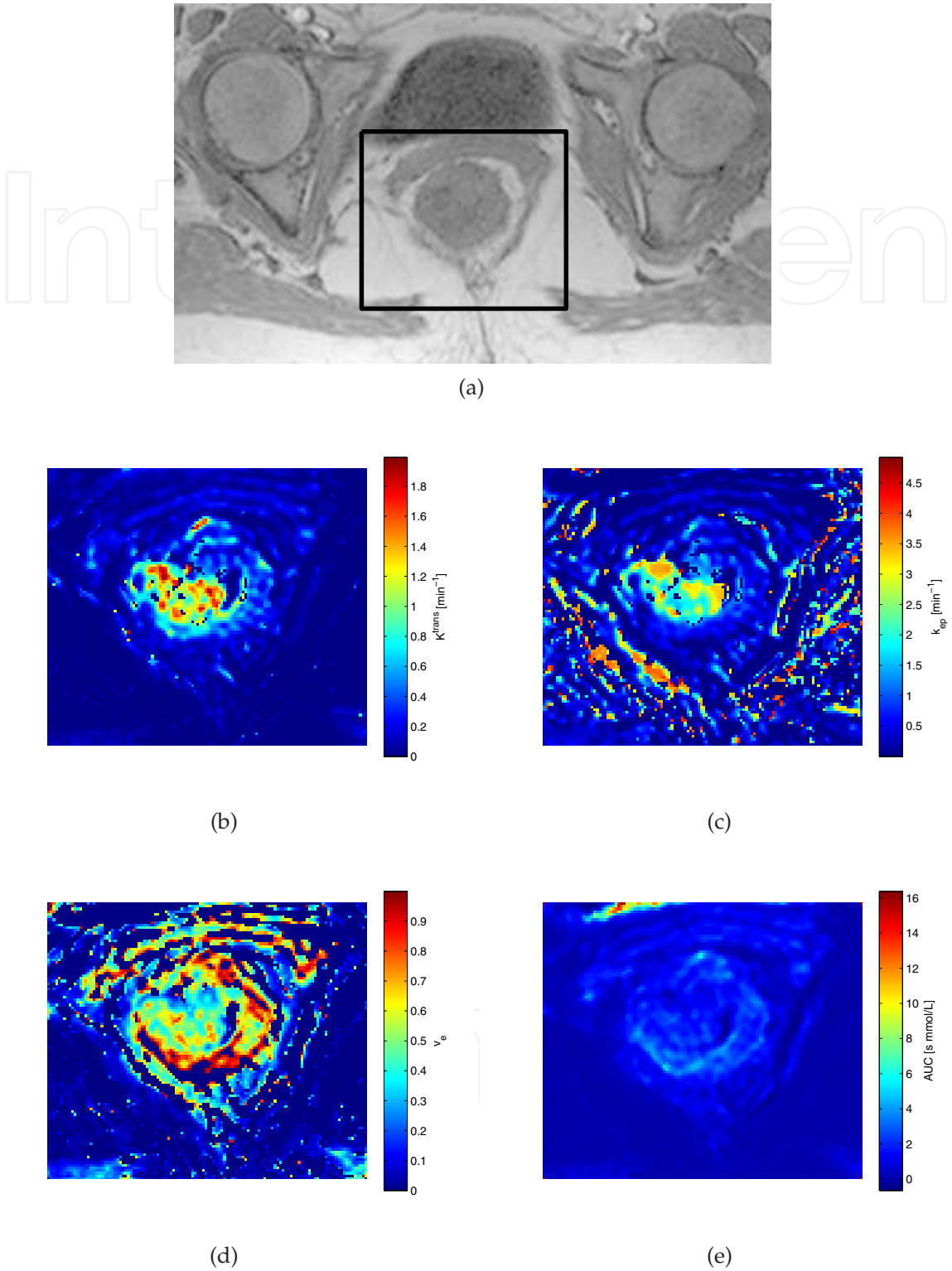
(a)

(b)

(c)

(d)

(e)

Fig. 7. Example of parametric maps. The pulse sequence had TE/TR/FlipAngle=4.76ms/9.8ms/25°, pixel resolution 0.6 x 0.6 mm x mm, sampling interval of 34 s. a) T_1-weighted image: the rectangle surrounds the ROI chosen by a radiologist; b) K^{trans} map; c) k_{ep} map; d) v_e map. e) Area under the Gd curve (AUC);

5. DCE-MRI in rectal cancer

In this section we will discuss a number of studies reporting findings concerning the application of DCE-MRI to rectal cancer. Mainly, DCE-MRI has been applied for both cancer staging and therapy response evaluation. Studies can be grouped according to the approach used: either semi-quantitative or full-quantitative (see section (4)).

As discussed in section (4), in principle, a full model-based approach should provide information directly related to vessels permeability and blood flow, thus evidencing vasculature modification caused by chemo-radiotherapy. However, drawbacks of this approach include: a great accuracy is required for gadolinium quantification; model choice is not always clear; parameters estimation is affected by the specific algorithm chosen. The semi-quantitative approach, instead, although providing summary information, roughly related to the patophysiology of the cancer, could be more robust in clinical settings.

Blomqvist et al. (1998) proposed a piecewise linear fitting of the TIC. The TIC was divided into three parts: the first part was characterised by the time needed for the contrast medium to reach the ROI; the second part was characterised by the rapid increase in signal intensity (wash-in); the third part presented little or no increase in CA. In their study, none of the parameters in the piecewise linear approximation were found to significantly help discriminating malignant from benign. WOI was the only parameter that was significantly different between the malignant and benign groups.

Preoperative TNM staging of rectal cancer using endorectal coil and dynamic contrast enhancement, was performed by Drew et al. (1999) using visual inspection based on the pattern of the enhancement: they found a substantial tumour over-staging when compared to pathological specimens.

Dicle et al. (1999) evaluated the accuracy of DCE-MRI in the differentiation of malignant and benign pelvic lesions during follow-up of patients with treated colorectal tumours, using a semi-quantitative approach. They calculated the maximum change in relative enhancement E_{max} (which is related to MSD), the acceleration rate of the TIC (which can be identified approximately as WIS) and the ratio of the signal intensity of the lesions to the signal intensity of the iliac artery at 60 s ($(S_L/S_A)_{60}$). The acceleration rate of the TIC and $(S_L/S_A)_{60}$ were found to be valuable in the differential diagnosis; E_{max} showed no capability to differentiate benign from malignant lesions. Sensitivity was 83% for each calculated parameter. $(S_L/S_A)_{60}$ had the highest specificity and accuracy among the parameters.

de Vries et al. (2000) have monitored 11 patients with cT3 rectal carcinoma who underwent preoperative chemoirradiation. They looked for a relationship between the PI (eq. 7) with therapy outcome. They used a short sampling interval of 14s in the wash-in phase (first 10 minutes of acquisition) followed by a longer interval (2 min) in the subsequent period (up to 50 min). They found that PI increased after the 1st and 2nd week of treatment. Monitoring of PI values before therapy seemed to have a prognostic value: they found a significant correlation between PI before therapy and N downstaging.

After, de Vries et al. (2001) evaluated 17 patients using a similar methodology. Moreover in this study they evaluated also the tumor heterogeneity. They found similar results.

Later, the same research group de Vries et al. (2003) observed further 34 patients with primary rectal carcinoma and preoperative chemoirradiation. They found that the PI of non-responders before therapy was higher than responders. They showed the possible role of an increased angiogenic activity in aggressive tumour cell clusters that resulted in reduced nutrient supply and higher fraction of intratumoral necrosis.

Study	Parameters	Final Diag.	Nr. Pat.	Nr. Imag
Blomqvist et al. (1998)	TTP, WIS, WOI, WOS	TNM	30	60
Drew et al. (1999)		TNM	29	
Dicle et al. (1999)	MSD, $(S_L/S_A)_{60}$	biopsy	19	
de Vries et al. (2000)	PI	TNM	11	31 + (15)
de Vries et al. (2001)	PI	TNM	17	
de Vries et al. (2003)	PI	TNM	34	31 + (15)
Kremser et al. (2007)	PI	TNM	58	15
Tuncbilek et al. (2004)	$MSD_{1min}, MSD, \%/s, TWI$	MVD	21	8
Zhang et al. (2008)	$ER_{peak}, TTP, T_{first}$, uptake rate	MVD,VEGF	38	15-20
Müller-Schimpfle et al. (1993)	K^{trans}, v_e	needle biopsy	18	24
George et al. (2001)	K^{trans}	VEGF	31	42
Torricelli et al. (2003)	relative enhanchement	biopsy/surgery	36	11-13
de Lussanet et al. (2005)	$K^{trans}, k_{ep}, v_e, PI$	MVD,CD31,CD34	17	250
Atkin et al. (2006)	K^{trans}, v_e, MSD	MVD,CD31,VEGF	14	40
Ceelen et al. (2006)	K^{trans}, v_e	MVD,VEGF,pO_2	11 (rats)	500
Mross et al. (2009)	K^{trans}, AUC	VEGF	22	106
Yao et al. (2011)	K^{trans}, v_e, k_{ep}	MVD,TNM	26	25
Gu et al. (2011)	K^{trans}, v_e, k_{ep}	TNM	26	10

Table 2. Summary of the main characteristics of the examined DCE-MRI rectal cancer studies. Per eac parameters examined; the method used for final diagnosis; the number of patients; the number of im between them.

In line with these results, the same researchers published another paper (Kremser et al., 2007) in which they examined, using similar methodology, 58 patients before chemo-radiotherapy . Once again they found that PI is a good predictor of therapy outcome, being, before therapy, the PI of non-responders lower than responders.

Torricelli et al. (2003) elaborated dynamic images with a semi-quantitative postprocessing by plotting TICs and calculating the percentage of signal increase at the end of the first postcontrast dynamic sequence. The pelvic lesions were classified as recurrent or not recurrent by applying the following diagnostic criteria: (a) morphology and signal intensity of the lesion in unenhanced sequences and (b) percentage of enhancement in dynamic enhanced sequences. Unenhanced MRI had 80% sensitivity and 86% specificity. Analysis of the percentage of enhancement showed 87% sensitivity and 100% specificity.

Tuncbilek et al. (2004) studied 21 consecutive patients without radiotherapy (RT). They observed that TTP, WII_{max} and $E_{max/1}$ were strong correlated with microvessel density (MVD). As regards prognostic value, they found that histologic grade and $E_{max/1}$ correctly predicted metastases in 66.7% and 90.5 % of cases respectively.

Using a 3T scanner and basing on a semi-quantitative approach Zhang et al. (2008) found that rectal carcinoma had higher ER_{peak}, higher uptake rate ER_{peak}/T_{peak}, earlier T_{peak}, earlier $T_{firstenhanceent}$, than normal rectal wall.

All the previous studies showed that a semi-quantitative approach is feasible and can have good performances. In particular the perfusion index (PI) has shown to be a simple and robust prognostic factor.

On the other side, general guidelines for tracer kinetics approach have been indicated by Leach et al. (2005). Primary (K^{trans}, AUC) and secondary (v_e, k_{ep}) endpoints have been recommended.

Tracer kinetics modelling has been applied to the rectal cancer by Müller-Schimpfle et al. (1993) who reported 91-100 % sensitivity in differentiating benign from malignant lesions in pelvic lesions. Furthermore, they demonstrated that malignant lesions showed faster and greater enhancement compared with benign lesions and claimed that a more accurate differentiation with the usage of dynamic gadolinium-enhanced MRI could be obtained than with standard contrast-enhanced MRI.

As regards the therapy response, George et al. (2001) showed a correlation between K_{trans} and VEGF tumour expression showing that tumours having higher permeability seemed to better respond to pre-CRT than tumours having lower permeability.

de Lussanet et al. (2005) evaluated radio-therapy related microvascular changes in locally advanced rectal cancer (LARC) by DCE-MRI quantitative approach and histology. This study showed that K^{trans} values presents significant radio-therapy related reductions in microvessel blood flow in locally advanced rectal cancer. They studied tumor heterogeneity using histograms of K^{trans}, v_e and evaluating medina tumor values and median tumor/muscle ratio. Radiation therapy damages all blood vessels, but specific effects depend on vessel size, location, and dose-time-volume factors. Although acute effects of RT are marked by increased microvascular permeability, related to endothelial cell damage and local inflammation, longer term effects are marked by decreased permeability, resulting from basement membrane thickening and extracapillary fibrosis. The DCE-MRI volume fraction EES (v_e) showed some increased variation after Rt. Cell destruction caused by radiation may have increased the relative EES to which the CA can leak. In other part of the tumor infiltration of inflammatory cells can decrease EES.
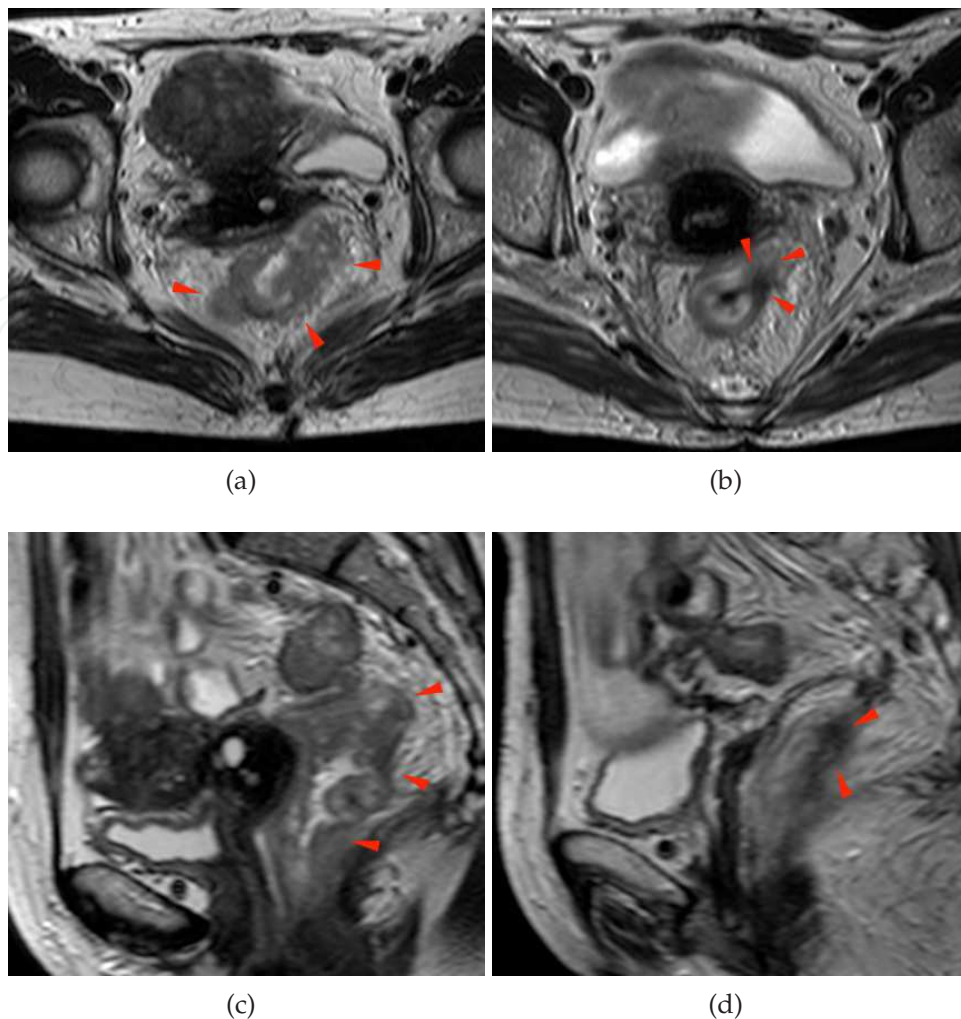
Fig. 8. (a) A heterogeneous irregular thickening along the entire rectal wall is well shown on T2w axial pre-pCRT scan (arrowheads). (b) After pCRT, a hypo-intense spiculated area with thin digitations into peri-rectal fat is visible on T2w axial scan (arrowheads). (c) In the same patient, multiple irregular rectal wall thickening are shown on T2w sagittal pre-pCRT scan (arrowheads). (d) A single hypo-intense area, showed also in (b) is pointed by arrowheads, suspecting for a residual post-pCRT tumor focus (arrowheads).

Controversially, Atkin et al. (2006) analysed 14, by preoperative DCE-MRI, patients that had not undergone any previous chemo-radioherapy. They reported a negative correlation between transfer constant K^{trans} with CD31. They noticed that this correlation is paradoxical because K^{trans} should be posiively coupled to blood flow,microvessel permeability and surface area. They suggested that this paradox could be related to the high level of maturation of vessels within rectal cancers, with mature vessels demonstrating relatively low permeability. Moreover, they reported no correlation of DCE-MRI with other measures such as MVD (which provide anatomical data only). Therefore they concluded that DCE-MRI does not simply reflect static histological vascular properties in patients with rectal cancer.

Monitoring 11 rats before and after fractionated short-term radiotherapy (Ceelen et al., 2006) observed a significant reduction of K^{trans} and v_e, while in non irradiated muscle tissue no changes were observed. After RT, pO_2 levels were inversely related to both K^{trans} and v_e. No

(a)   (b)

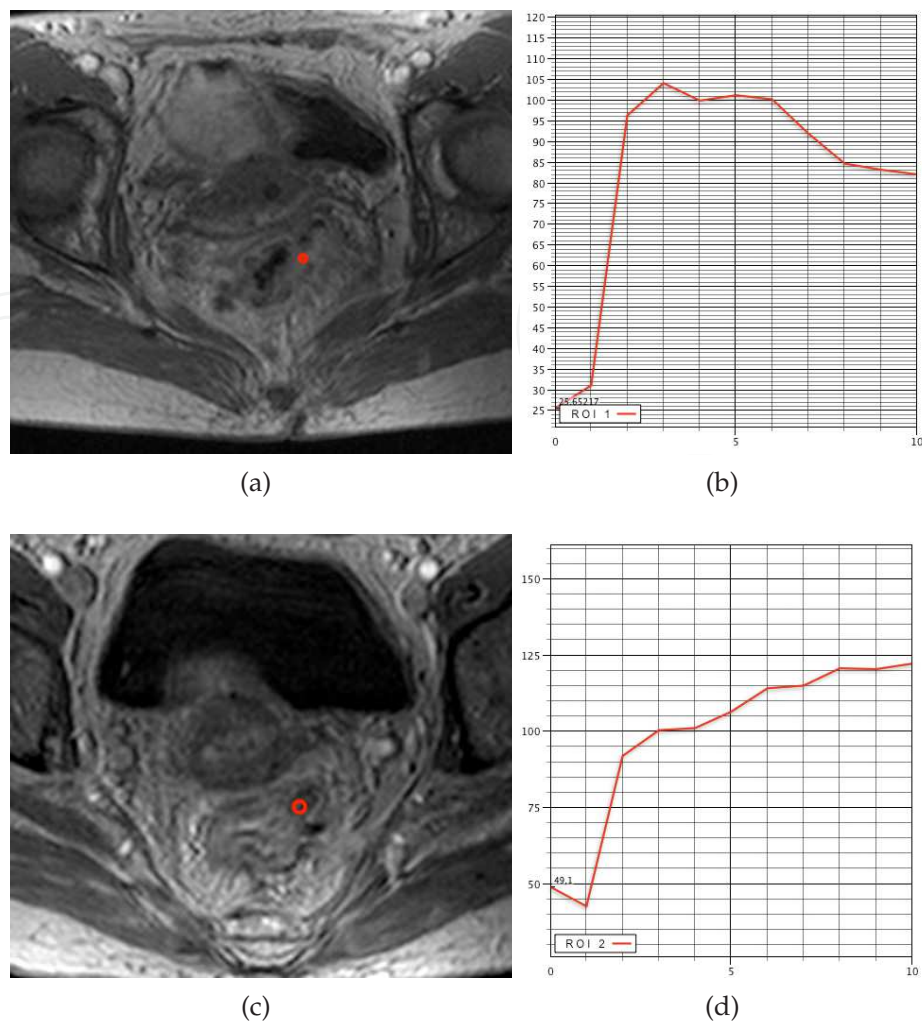(c)   (d)

Fig. 9. T1w post-contrast scan obtained on the same patient in fig. 8, before (a)-(b) and after (c)-(d) pre-CRT. The analysis of TIC calculated on a ROI, drawn outside the rectal wall where on T2w scans (fig. 8) tumor clearly spreads into peri-rectal fat pad, confirm this suspect showing a rapid CA intake and a fast discharge (b). After pre-CRT, on the same areas showed on T2w scans (fig. 8) no pathological CA uptake is present confirming that hypo-intense tissue visible on T2w scans are tumor nests but only residual inflammation due to pre-CRT. This patient was considered as a Responder. Histopathology showed a TRG 1.

correlation was found between DCE-MRI parameters and histologic parameters (MVD, VEGF expression). MVD did not differ significantly between RT-trated and control animals.

Mross et al. (2009) proposed an hybrid approach including AUC and K^{trans} for evaluating the response to treatment of 22 patients.

Yao et al. (2011) reported moderate and strong relationship between K^{trans} and clinicopathological elements, K^{trans} might be the prognostic indicator of rectal cancer.

Gu et al. (2011) found a positive correlations between k_{ep} and SUV values in primary rectal adenocarcinomas suggesting an association between angiogenesis and metabolic activity and further reflecting that angiogenic activity in washout phase is better associated with tumor metabolism than the uptake phase.

Although these encouraging results, the evaluation after neo-adjuvant therapy remains actually difficult in borderline cases where an overestimation is the most common drawback.

This phenomenon has been addressed to the presence of inflammatory tissue still mostly vascularized so as tumour residual areas (see fig. 8 and 9).

In conclusion, DCE-MRI can be considered a valuable tool for clinical investigation of rectal cancer, in particular for re-staging and therapy evaluation. Further improvements should involve the underestimation phenomenon, a clinically relevant problem, frequently observed on morphologic MRI that is not yet been solved because of the presence of small areas of tumors within poorly vascularized fibrotic tissue under the spatial resolution of DCE-MRI technique.

6. References

Ashton, E. (2010). Quantitative MR in multi-center clinical trials, *J Magn Reson Imaging* 31(2): 279–288.

Atkin, G., Taylor, N. J., Daley, F. M., Stirling, J. J., Richman, P., Glynne-Jones, R., d'Arcy, J. A., Collins, D. J. & Padhani, A. R. (2006). Dynamic contrast-enhanced magnetic resonance imaging is a poor measure of rectal cancer angiogenesis, *Brit J Surg* 93(8): 992–1000.

Avallone, A., Delrio, P., Guida, C., Tatangelo, F., Petrillo, A., Marone, P., Cascini, L. G., Morrica, B., Lastoria, S., Parisi, V., Budillon, A. & Comella, P. (2006). Biweekly oxaliplatin, raltitrexed, 5-fluorouracil and folinic acid combination chemotherapy during preoperative radiation therapy for locally advanced rectal cancer: a phase I-II study, *Brit J Cancer* 94(12): 1809–1815.

Avallone, A., Delrio, P., Pecori, B., Tatangelo, F., Petrillo, A., Scott, N., Marone, P., Aloi, L., Sandomenico, C., Lastoria, S., Iaffaioli, V. R., Scala, D., Iodice, G., Budillon, A. & Comella, P. (2011). Oxaliplatin plus dual inhibition of thymidilate synthase during preoperative pelvic radiotherapy for locally advanced rectal carcinoma: long-term outcome, *Int J Radiat Oncol* 79(3): 670–676.

Beets-Tan, R. G. H. & Beets, G. L. (2004). Rectal cancer: review with emphasis on MR imaging, *Radiology* 232(2): 335–346.

Blomqvist, L., Fransson, P. & Hindmarsh, T. (1998). The pelvis after surgery and radio-chemotherapy for rectal cancer studied with Gd-DTPA-enhanced fast dynamic MR imaging, *Eur Radiol* 8(5): 781–787.

Brix, G., Griebel, J., Kiessling, F. & Wenz, F. (2010). Tracer kinetic modelling of tumour angiogenesis based on dynamic contrast-enhanced CT and MRI measurements, *Eur J Nucl Med Mol Imaging* 37 Suppl 1: S30–51.

Brix, G., Semmler, W., Port, R., Schad, L. R., Layer, G. & Lorenz, W. J. (1991). Pharmacokinetic parameters in CNS Gd-DTPA enhanced MR imaging, *J Comput Assist Tomogr* 15(4): 621–628.

Buonaccorsi, G. A., O'Connor, J. P., Caunce, A., Roberts, C., Cheung, S., Watson, Y., Davies, K., Hope, L., Jackson, A., Jayson, G. C. & Parker, G. J. (2007). Tracer kinetic model–driven registration for dynamic contrast-enhanced MRI time-series data, *Magnet Reson Med* 58(5): 1010–1019.

Ceelen, W., Smeets, P., Backes, W., Damme, N. V., Boterberg, T., Demetter, P., Bouckenooghe, I., Visschere, M. D., Peeters, M. & Pattyn, P. (2006). Noninvasive monitoring of radiotherapy-induced microvascular changes using dynamic contrast enhanced magnetic resonance imaging (DCE-MRI) in a colorectal tumor model, *Int J Radiat Oncol* 64(4): 1188–1196.

Chen, C., Lee, R., Lin, J., Wang, L. & Yang, S. (2005). How accurate is magnetic resonance imaging in restaging rectal cancer in patients receiving preoperative combined chemoradiotherapy?, *Dis Colon Rectum* 48(4): 722–728.

Cheng, H. M. (2008). Investigation and optimization of parameter accuracy in dynamic contrast-enhanced MRI, *J Magn Reson Imaging* 28(3): 736–743.

Choyke, P. L., Dwyer, A. J. & Knopp, M. V. (2003). Functional tumor imaging with dynamic contrast-enhanced magnetic resonance imaging, *J Magn Reson Imaging* 17(5): 509–520.

Collins, D. J. & Padhani, A. R. (2004). Dynamic magnetic resonance imaging of tumor perfusion, *IEEE Eng Med Biol Mag* 23(5): 65– 83.

Dale, B. M., Jesberger, J. A., Lewin, J. S., Hillenbrand, C. M. & Duerk, J. L. (2003). Determining and optimizing the precision of quantitative measurements of perfusion from dynamic contrast enhanced MRI, *J Magn Reson Imaging* 18(5): 575–584.

Daniel, B. L., Yen, Y. F., Glover, G. H., Ikeda, D. M., Birdwell, R. L., Sawyer-Glover, A. M., Black, J. W., Plevritis, S. K., Jeffrey, S. S. & Herfkens, R. J. (1998). Breast disease: dynamic spiral MR imaging, *Radiology* 209(2): 499–509.

de Lussanet, Q. G., Backes, W. H., Griffioen, A. W., Padhani, A. R., Baeten, C. I., van Baardwijk, A., Lambin, P., Beets, G. L., van Engelshoven, J. M. A. & Beets-Tan, R. G. H. (2005). Dynamic contrast-enhanced magnetic resonance imaging of radiation therapy-induced microcirculation changes in rectal cancer, *Int J Radiat Oncol* 63(5): 1309–1315.

de Vries, A. F., Griebel, J., Kremser, C., Judmaier, W., Gneiting, T., Debbage, P., Kremser, T., Pfeiffer, K. P., Buchberger, W. & Lukas, P. (2000). Monitoring of tumor microcirculation during fractionated radiation therapy in patients with rectal carcinoma: preliminary results and implications for therapy, *Radiology* 217(2): 385–391.

de Vries, A. F., Griebel, J., Kremser, C., Judmaier, W., Gneiting, T., Kreczy, A., Ofner, D., Pfeiffer, K. P., Brix, G. & Lukas, P. (2001). Tumor microcirculation evaluated by dynamic magnetic resonance imaging predicts therapy outcome for primary rectal carcinoma, *Cancer Res* 61(6): 2513–2516.

de Vries, A. F., Kremser, C., Hein, P. A., Griebel, J., Krezcy, A., Ofner, D., Pfeiffer, K. P., Lukas, P. & Judmaier, W. (2003). Tumor microcirculation and diffusion predict therapy outcome for primary rectal carcinoma, *Int J Radiat Oncol* 56(4): 958–965.

Delrio, P., Avallone, A., Guida, C., Lastoria, S., Tatangelo, F., Cascini, G. M., Marone, P., Petrillo, A., Budillon, A., Marzo, M. D., Palaia, R., Albino, V., Rosa, V. D. & Parisi, V. (2005). Multidisciplinary approach to locally advanced rectal cancer: results of a single institution trial, *Suppl Tumori* 4(3): S8.

Delrio, P., Lastoria, S., Avallone, A., Ravo, V., Guida, C., Cremona, F., Izzo, F., Palaia, R., Ruffolo, F., Puppio, B., Guidetti, G. M., Cascini, G. L., Casaretti, R., Tatangelo, F., Marone, P., Rossi, G. B., Budillon, A., Petrillo, A., Rosa, V. D., Comella, G., Morrica, B., Tempesta, A., Botti, G. & Parisi, V. (2003). Early evaluation using PET-FDG of the efficiency of neoadjuvant radiochemotherapy treatment in locally advanced neoplasia of the lower rectum, *Tumori* 89(4 Suppl): 50–53.

Dicle, O., Obuz, F. & Cakmakci, H. (1999). Differentiation of recurrent rectal cancer and scarring with dynamic MR imaging, *Brit J Radiol* 72(864): 1155–1159.

Dor, Y., Porat, R. & Keshet, E. (2001). Vascular endothelial growth factor and vascular adjustments to perturbations in oxygen homeostasis, *Am J Physiol Cell Physiol* 280(6): C1367–1374.

Drew, P. J., Farouk, R., Turnbull, L. W., Ward, S. C., Hartley, J. E. & Monson, J. R. (1999). Preoperative magnetic resonance staging of rectal cancer with an endorectal coil and dynamic gadolinium enhancement, *Brit J Surg* 86(2): 250–254.

Evelhoch, J. L. (1999). Key factors in the acquisition of contrast kinetic data for oncology, *J Magn Reson Imaging* 10(3): 254–259.

Fei, B., Wheaton, A., Lee, Z., Duerk, J. L. & Wilson, D. L. (2002). Automatic MR volume registration and its evaluation for the pelvis and prostate, *Phys Med Biol* 47(5): 823–838.

George, M. L., Dzik-Jurasz, A. S., Padhani, A. R., Brown, G., Tait, D. M., Eccles, S. A. & Swift, R. I. (2001). Non-invasive methods of assessing angiogenesis and their value in predicting response to treatment in colorectal cancer, *Brit J Surg* 88(12): 1628–1636.

Goh, V., Padhani, A. R. & Rasheed, S. (2007). Functional imaging of colorectal cancer angiogenesis, *Lancet Oncol* 8(3): 245–255.

Gu, J., Khong, P., Wang, S., Chan, Q., Wu, E. X., Law, W., Liu, R. K. & Zhang, J. (2011). Dynamic contrast-enhanced MRI of primary rectal cancer: quantitative correlation with positron emission tomography/computed tomography, *J Magn Reson Imaging* 33(2): 340–347.

Guetz, G. D., Uzzan, B., Nicolas, P., Cucherat, M., Morere, J., Benamouzig, R., Breau, J. & Perret, G. (2006). Microvessel density and VEGF expression are prognostic factors in colorectal cancer. meta-analysis of the literature, *Brit J Cancer* 94(12): 1823–1832.

Gunderson, L. L., Sargent, D. J., Tepper, J. E., O'Connell, M. J., Allmer, C., Smalley, S. R., Martenson, J. A., Haller, D. G., Mayer, R. J., Rich, T. A., Ajani, J. A., Macdonald, J. S. & Goldberg, R. M. (2002). Impact of T and N substage on survival and disease relapse in adjuvant rectal cancer: a pooled analysis, *Int J Radiat Oncol* 54(2): 386–396.

Gunderson, L. L., Sargent, D. J., Tepper, J. E., Wolmark, N., O'Connell, M. J., Begovic, M., Allmer, C., Colangelo, L., Smalley, S. R., Haller, D. G., Martenson, J. A., Mayer, R. J., Rich, T. A., Ajani, J. A., MacDonald, J. S., Willett, C. G. & Goldberg, R. M. (2004). Impact of T and N stage and treatment on survival and relapse in adjuvant rectal cancer: a pooled analysis, *J Clin Oncol* 22(10): 1785–1796.

Henderson, E., Rutt, B. K. & Lee, T. (1998). Temporal sampling requirements for the tracer kinetics modeling of breast disease, *Magn Reson Imaging* 16(9): 1057–1073.

Jackson, A., O'Connor, J. P. B., Parker, G. J. M. & Jayson, G. C. (2007). Imaging tumor vascular heterogeneity and angiogenesis using dynamic contrast-enhanced magnetic resonance imaging, *Clin Cancer Res* 13(12): 3449–3459.

Kapse, N. & Goh, V. (2009). Functional imaging of colorectal cancer: positron emission tomography, magnetic resonance imaging, and computed tomography, *Clin Colorectal Cancer* 8(2): 77–87.

Kelm, B., Menze, B., Nix, O., Zechmann, C. & Hamprecht, F. (2009). Estimating kinetic parameter maps from dynamic Contrast-Enhanced MRI using spatial prior knowledge, *IEEE Trans Med Imaging* 28(10): 1534–1547.

Kety, S. S. (1951). The theory and applications of the exchange of inert gas at the lungs and tissues, *Pharmacol Rev* 3(1): 1–41.

Knopp, M. V., Weiss, E., Sinn, H. P., Mattern, J., Junkermann, H., Radeleff, J., Magener, A., Brix, G., Delorme, S., Zuna, I. & van Kaick, G. (1999). Pathophysiologic basis of contrast enhancement in breast tumors, *J Magn Reson Imaging* 10(3): 260–266.

Kremser, C., Trieb, T., Rudisch, A., Judmaier, W. & de Vries, A. (2007). Dynamic t(1) mapping predicts outcome of chemoradiation therapy in primary rectal carcinoma: sequence implementation and data analysis, *J Magn Reson Imaging* 26(3): 662–671.

Kuhl, C. (2007). The current status of breast MR imaging part i. choice of technique, image interpretation, diagnostic accuracy, and transfer to clinical practice, *Radiology* 244(2): 356 –378.

Larsson, H. B. W., Fritz-Hansen, T., Rostrup, E., Sondergaard, L., Ring, P. & Henriksen, O. (1996). Myocardial perfusion modeling using MRI, *Magnet Reson Med* 35(5): 716–726.

Leach, M. O., Brindle, K. M., Evelhoch, J. L., Griffiths, J. R., Horsman, M. R., Jackson, A., Jayson, G. C., Judson, I. R., Knopp, M. V., Maxwell, R. J., McIntyre, D., Padhani, A. R., Price, P., Rathbone, R., Rustin, G. J., Tofts, P. S., Tozer, G. M., Vennart, W., Waterton, J. C., Williams, S. R. & Workman, P. (2005). The assessment of antiangiogenic and antivascular therapies in early-stage clinical trials using magnetic resonance imaging: issues and recommendations, *Brit J Cancer* 92(9): 1599–1610.

Lichtenbeld, H. C., Ferarra, N., Jain, R. K. & Munn, L. L. (1999). Effect of local anti-VEGF antibody treatment on tumor microvessel permeability, *Microvasc Res* 57(3): 357–362.

Melbourne, A., Atkinson, D., White, M. J., Collins, D., Leach, M. & Hawkes, D. (2007). Registration of dynamic contrast-enhanced MRI using a progressive principal component registration (PPCR), *Phys Med Biol* 52(17): 5147–5156.

Miles, K. A. (1991). Measurement of tissue perfusion by dynamic computed tomography, *Brit J Radiol* 64(761): 409–412.

Müller-Schimpfle, M., Brix, G., Layer, G., Schlag, P., Engenhart, R., Frohmuller, S., Hess, T., Zuna, I., Semmler, W. & van Kaick, G. (1993). Recurrent rectal cancer: diagnosis with dynamic MR imaging, *Radiology* 189(3): 881–889.

Mross, K., Fasol, U., Frost, A., Benkelmann, R., Kuhlmann, J., Büchert, M., Unger, C., Blum, H., Hennig, J., Milenkova, T. P., Tessier, J., Krebs, A. D., Ryan, A. J. & Fischer, R. (2009). DCE-MRI assessment of the effect of vandetanib on tumor vasculature in patients with advanced colorectal cancer and liver metastases: a randomized phase i study, *J Angiogenes Res* 1: 5.

Nishiura, M., Yasuhiro, T. & Murase, K. (2011). Evaluation of time-intensity curves in ductal carcinoma in situ (DCIS) and mastopathy obtained using dynamic contrast-enhanced magnetic resonance imaging, *Magn Reson Imaging* 29(1): 99–105.

Orton, M. R., d'Arcy, J. A., Walker-Samuel, S., Hawkes, D. J., Atkinson, D., Collins, D. J. & Leach, M. O. (2008). Computationally efficient vascular input function models for quantitative kinetic modelling using DCE-MRI, *Phys Med Biol* 53(5): 1225–1239.

Parker, G. J. M., Roberts, C., Macdonald, A., Buonaccorsi, G. A., Cheung, S., Buckley, D. L., Jackson, A., Watson, Y., Davies, K. & Jayson, G. C. (2006). Experimentally-derived functional form for a population-averaged high-temporal-resolution arterial input function for dynamic contrast-enhanced MRI, *Magnet Reson Med* 56(5): 993–1000.

Parker, G. J., Suckling, J., Tanner, S. F., Padhani, A. R., Revell, P. B., Husband, J. E. & Leach, M. O. (1997). Probing tumor microvascularity by measurement, analysis and display of contrast agent uptake kinetics, *J Magn Reson Imaging* 7(3): 564–574.

Petrillo, A., Catalano, O., Delrio, P., Avallone, A., Guida, C., Filice, S. & Siani, A. (2007). Post-treatment fistulas in patients with rectal cancer: MRI with rectal superparamagnetic contrast agent, *Abdom Imaging* 32(3): 328–331.

Petrillo, A., Filice, S., Avallone, A., Delrio, P., Guida, C., Tatangelo, F., Marone, P., Nunziata, A. & Siani, A. (2006). Staging of locally advanced rectal cancer (LARC): proposal of

a one-stop magnetic resonance (mr) imaging-based protocol, *Eur Radiol Supplements* 16: 321–494.

Sansone, M., Fusco, R., Petrillo, A., Petrillo, M. & Bracale, M. (2011). An expectation-maximisation approach for simultaneous pixel classification and tracer kinetic modelling in dynamic contrast enhanced-magnetic resonance imaging, *Med Biol Eng Comput* 49(4): 485–495.

Schmid, V. J., Whitcher, B., Padhani, A. R., Taylor, N. J. & Yang, G. (2006). Bayesian methods for pharmacokinetic models in dynamic Contrast-Enhanced magnetic resonance imaging, *IEEE Transactions on Medical Imaging* 25(12): 1627–1636.

Simpson, N. E., He, Z. & Evelhoch, J. L. (1999). Deuterium NMR tissue perfusion measurements using the tracer uptake approach: I. optimization of methods, *Magnet Reson Med* 42(1): 42–52.

Sourbron, S. (2010). Technical aspects of MR perfusion, *Eur J Radiol* 76(3): 304–313.

St Lawrence, K. S. & Lee, T. Y. (1998). An adiabatic approximation to the tissue homogeneity model for water exchange in the brain: I. theoretical derivation, *J Cereb Blood Flow Metab* 18(12): 1365–1377.

Stanisz, G. J. & Henkelman, R. M. (2000). Gd-DTPA relaxivity depends on macromolecular content, *Magnet Reson Med* 44(5): 665–667.

Tofts, P. S. (1997). Modeling tracer kinetics in dynamic Gd-DTPA MR imaging, *J Magn Reson Imaging* 7(1): 91–101.

Tofts, P. S., Brix, G., Buckley, D. L., Evelhoch, J. L., Henderson, E., Knopp, M. V., Larsson, H. B., Lee, T. Y., Mayr, N. A., Parker, G. J., Port, R. E., Taylor, J. & Weisskoff, R. M. (1999). Estimating kinetic parameters from dynamic contrast-enhanced t(1)-weighted MRI of a diffusable tracer: standardized quantities and symbols, *J Magn Reson Imaging* 10(3): 223–232.

Torricelli, P., Pecchi, A., Luppi, G. & Romagnoli, R. (2003). Gadolinium-enhanced MRI with dynamic evaluation in diagnosing the local recurrence of rectal cancer, *Abdom Imaging* 28(1): 19–27.

Tuncbilek, N., Karakas, H. M. & Altaner, S. (2004). Dynamic mri in indirect estimation of microvessel density, histologic grade, and prognosis in colorectal adenocarcinomas, *Abdom Imaging* 29: 166–172.

Walker-Samuel, S., Leach, M. O. & Collins, D. J. (2007). Reference tissue quantification of DCE-MRI data without a contrast agent calibration, *Phys Med Biol* 52(3): 589–601.

Weinmann, H. J., Laniado, M. & Mützel, W. (1984). Pharmacokinetics of GdDTPA/dimeglumine after intravenous injection into healthy volunteers, *Physiol Chem Phys Med NMR* 16(2): 167–172.

Xiaohua, C., Brady, M., Lo, J. L. & Moore, N. (2005). Simultaneous segmentation and registration of contrast-enhanced breast MRI, *Information Processing in Medical Imaging: Proceedings of the ... Conference* 19: 126–137.

Yang, C., Karczmar, G. S., Medved, M. & Stadler, W. M. (2004). Estimating the arterial input function using two reference tissues in dynamic contrast-enhanced MRI studies: Fundamental concepts and simulations, *Magnet Reson Med* 52(5): 1110–1117.

Yankeelov, T. E., Luci, J. J., Lepage, M., Li, R., Debusk, L., Lin, P. C., Price, R. R. & Gore, J. C. (2005). Quantitative pharmacokinetic analysis of DCE-MRI data without an arterial input function: a reference region model, *Magnet Reson Imaging* 23(4): 519–529.

Yao, W. W., Zhang, H., Ding, B., Fu, T., Jia, H., Pang, L., Song, L., Xu, W., Song, Q., Chen, K. & Pan, Z. (2011). Rectal cancer: 3D dynamic contrast-enhanced MRI; correlation with microvascular density and clinicopathological features, *Radiol Med* 116(3): 366–374.

Zhang, X. M., Yu, D., Zhang, H. L., Dai, Y., Bi, D., Liu, Z., Prince, M. R. & Li, C. (2008). 3D dynamic contrast-enhanced MRI of rectal carcinoma at 3T: correlation with microvascular density and vascular endothelial growth factor markers of tumor angiogenesis, *J Magn Reson Imaging* 27(6): 1309–1316.
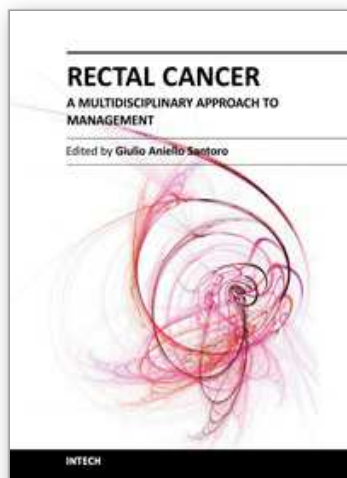
Rectal Cancer - A Multidisciplinary Approach to Management

Edited by Dr. Giulio A. Santoro

ISBN 978-953-307-758-1

Hard cover, 410 pages

Publisher InTech

Published online 10, October, 2011

Published in print edition October, 2011

Dramatic improvements in medicine over the last few years have resulted in more reliable and accessible diagnostics and treatment of rectal cancer. Given the complex physiopathology of this tumor, the approach should not be limited to a single specialty but should involve a number of specialties (surgery, gastroenterology, radiology, biology, oncology, radiotherapy, nuclear medicine, physiotherapy) in an integrated fashion. The subtitle of this book "A Multidisciplinary Approach to Management" encompasses this concept. We have endeavored, with the help of an international group of contributors, to provide an up-to-date and authoritative account of the management of rectal tumor.

How to reference

In order to correctly reference this scholarly work, feel free to copy and paste the following:

Roberta Fusco, Mario Sansone, Mario Petrillo, Antonio Avallone, Paolo Delrio and Antonella Petrillo (2011). Dynamic Contrast Enhanced Magnetic Resonance Imaging in Rectal Cancer, Rectal Cancer - A Multidisciplinary Approach to Management, Dr. Giulio A. Santoro (Ed.), ISBN: 978-953-307-758-1, InTech, Available from: http://www.intechopen.com/books/rectal-cancer-a-multidisciplinary-approach-to-management/dynamic-contrast-enhanced-magnetic-resonance-imaging-in-rectal-cancer

INTECH
open science | open minds